The calibration of NOAA-AVHRR visible radiances with VIRS

D. R. Doelling, V. Chakrapani
Analytical Services and Materials, Inc., Hampton, VA

Patrick Minnis and Louis Nguyen
Atmospheric Sciences, NASA-Langley Research Center, Hampton, VA

Proceedings AMS 11th Conference on Satellite Meteorology and Oceanography
Madison, Wisconsin
October 15 – 18, 2001
pp. 614-617

P5.29 The Calibration of NOAA AVHRR Visible Radiances with VIRS

David R. Doelling, Venkatesan Chakrapani
Analytical Services & Materials Inc., Hampton, VA

Patrick Minnis and Louis Nguyen
NASA Langley Research Center, Hampton, VA

1. INTRODUCTION

There is a long history of Advanced Very High Resolution Radiometer (AVHRR) derived products that rely on accurate visible channel radiances. Currently AVHRR instruments lack onboard calibration for channels 1 (0.65 µm) and 2 (0.87 µm). Operationally, these channels are calibrated using a stable desert surface target as a reference to account for degradation of the sensors (Rao and Chen 1999 and 1996; http://psbsgi1.nesdis.noaa.gov:8080/EBB/ml/niccal.html). Adjustments usually consist of a gain change that varies linearly with the day since launch of the particular satellite. Two NOAA satellites with AVHRR are usually operating at any given time: one is an afternoon (1330 or 1430 local equator crossing time (ECT)) and the other morning (0730 ECT) Sun-synchronous orbit. Operational calibrations are only performed for the afternoon orbiter. Degradation rates have been computed for NOAA-9 (Loeb 1997); 9, 10, and 11 (Masonis and Warren 2001); and 14 (Tahnk and Coakley 2001) using polar snow targets. For detection of long term trends in remotely sensed parameters and to detect changes in surface or cloud properties over a given location, it is critical to have consistent calibrations over the record of observations from satellite imagers. The polar inter-calibration technique can be used to determine the relative degradation between any two satellites. Thus, given enough overlap, a single calibration reference can be transferred from one satellite pair to the next to provide a consistent calibration for all available AVHRR data. This paper presents preliminary gain comparisons of sequential afternoon and morning satellites from NOAA-9 to NOAA-15 and they are normalized to a well-calibrated reference satellite imager.

Recently launched scanning radiometers, including the Moderate Resolution Imaging Spectroradiometer (MODIS), Visible Infrared Scanner (VIRS) and Along Track Scanning Radiometer (ATSR-2) use solar diffusers to calibrate their visible radiances. If these calibrations are reliable and the spectral response functions similar, then one could inter-calibrate VIRS, MODIS and ATSR-2 with AVHRR. It has been shown that VIRS has a stable visible calibration when compared with ATSR-2, MODIS, and other geostationary satellites (Minnis et. al. 2001). This paper uses the VIRS data as a reference for the NOAA-14 AVHRR visible channel that will be used to intercalibrate the AVHRRs on the other NOAA satellites. The direct AVHRR-VIRS calibrations are compared with an indirect 3-way calibration using matched VIRS and Geostationary Operational Environmental Satellite (GOES-8) data and AVHRR-GOES calibration. This 3-way calibration provides an estimate of the uncertainty resulting from a given satellite-to-satellite calibration transfer.

* *Corresponding Author Address*: D. R. Doelling, AS&M Inc., 1 Enterprise Parkway, Hampton, VA 23666; e-mail: d.r.doelling@larc.nasa.gov

2. NOAA Cross-Calibration Method

AVHRR Global Area Coverage (GAC) data were used for each satellite. To minimize errors, only coincident, collocated and angle-matched radiances were used to compare visible radiances from different satellite platforms. The best opportunities for meeting such criteria for a pair of afternoon and morning polar orbiters occur over polar regions. Their ground tracks only intersect at 80° north (1000 LST) or south (2200 LST) latitude 14 times a day. During the 8-day satellite repeat cycle, the time difference between the morning and afternoon satellite intersections ranges from 0 up to 45 minutes, the time required to complete half an orbit. Daytime intersections occur in the Northern Hemisphere from February until November; while during the remainder of the year the daytime intersections occur over the Southern Hemisphere. For this study, two days (8 days apart) of intersections are used, when the time difference is less than 2.5 minutes. These days straddle Dec. 23, Apr. 23, June 23, and Aug. 23. The solar zenith angles *(SZA)*, 77°, 67°, 57° and 67°, vary interannually by less than 3° for each month, despite the gradual precession of the ECT for each satellite.

For each intersection, several matched data points were created by computing the average 10-bit visible count over selected areas defined by a nominal radius of 50 km from the center of each matched region to minimize the effects of any navigation errors from either one or both of the satellites. These averages are based on approximately 150 pixels from each satellite. Usually, the counts are linearly related to radiance. For the one exception, NOAA-15, the dual-gain counts were first converted to radiances and then converted to NOAA-14 equivalent counts with the nominal calibration to provide a linear fit between counts and gain.

Several data points are possible for each intersection because the satellites cross at an angle of

~60° (or 120°). In addition to the matching nadir point, the viewing zenith angles *(VZA)* between the two satellites are equal at four different locations, one in each of the quadrants defined by the crossing orbital ground tracks. To differentiate between the matched *VZA*s in the oblique and acute crossing-angle quadrants, the lines between the ground track and the matching regions in the acute angle quadrants are referred to as the along-track. Similarly, the lines in the oblique-angle quadrants are denoted as cross-track lines. The radius was increased with *VZA* to ensure that at least 150 pixels were included in each data point. Only non-overlapping matched regions with *VZA* < 6° for along track and *VZA* < 17° in the cross-track were used for the off-nadir points. This matching approach results in more than one data point for each quadrant because the matched *VZA*s vary continuously with distance from the ground-track intersection. Although the relative azimuth angles *(RAZ)* differ for each satellite, the impact should be relatively small because the *VZA* are so small.

Figure 1 shows scatter plots of NOAA-11 and 12 channel 1 data of the off-nadir and nadir points from taken during December 1991 near the South Pole. Regressions were performed for each dataset using the force-fit and Principal Components (PC) methods. The force-fit technique holds the offset or space count constant at 41 and derives the slope from the mean radiances. The PC fit is essentially the first-order principal component and computes the minimum distance perpendicular to the line, thereby taking into account errors in both variables. The PC gain and offset for the data in Fig. 1a are 0.950 and 0.74 with the correlation coefficient r^2 = 0.994. The force-fit gain is 0.940 for 224 samples. The corresponding PC statistics for the nadir points are 0.887, 11.24, and 0.975 while the force-fit gain is 0.939 for 25 samples. The cross- and along-track points increased the dynamic range and the PC slope was similar to the force fit unlike the nadir case and the offset was near zero. Note the force fits in Fig. 1a and b are nearly the same.

Figure 2 shows the relative trend lines using both techniques applied to data from channels 1 and 2 for the five morning and afternoon satellite combinations. The trend lines have been normalized so that the mean of both the nadir and cross & along track monthly points is unity for the five satellite combinations. The trend line describes, for each satellite pair X-Y, the ratio of the gain drift of satellite Y to the gain drift of satellite X. Thus the first set of lines in the top panel of Fig. 2 is for the ratios of the NOAA-10 to the NOAA-9 gains. Gaps in time series are found for January and December 1995 and Dec 1989. Those data were not used because the PC offset was greater than 20 counts suggesting too much noise in the data. The PC gain and offset drifts usually occur in tandem with one coefficient offsetting the effect of the other. The force fit is not really affected by any apparent space count drifts. The relative gain for the South Pole data often differs from that from the North Pole. These pole-to-pole changes are mostly balanced by changes in the offsets. The reason for the hemispherical variation may be related to differences in the *RAZ*s.

The force fit plots in Fig. 2 show that the nadir and cross- and along-track trend lines are nearly identical except for NOAA-12 and 14. This suggests that the cross and along track points do not bias the slope and that the *VZA* limitations eliminate most of the impact from differing *RAZ*s. The off-nadir PC and force-fit slopes for NOAA-12/NOAA-14 are systematically below the nadir counterparts. This anomaly may be due to different geometry between the two satellites relative to the other four pairs. More study is required to understand these differences.

Overall, the relative gain trends appear to be linear. Negative trends indicate that the newer satellite is degrading faster than the older satellite. The only positive trends occur for the NOAA-9/NOAA-10 combination and for the NOAA-14/NOAA-15 channel 2 gains. Masonis and Warren (2001) found that NOAA-10 degraded in a cyclical fashion with the gain decreasing before November 1988 and increasing afterwards. Although channels 1 and 2 do not degrade in the same fashion, they generally degrade in the same direction relative to the other satellite. The exception again is for the NOAA-14/NOAA-15 combination. These relative gain drifts will be compared with published calibrations such as Masonis and Warren (2001) and Brest et. al. (1997) for verification.

3. VIRS and NOAA-14 Inter-calibration

Absolute values for each of the gains will be assigned by first normalizing the NOAA-14 gains to the VIRS, then transferring the gains using the relative trend lines in Fig. 2. VIRS is operating on the Tropical Rainfall Measuring Mission (TRMM) satellite that was launched in November 1997 into a 35° precessing orbit. To effect the matching of NOAA-14 and VIRS, an orbital prediction routine was used to locate intersections within 15 min for the NOAA-14 and TRMM ground tracks. A 40 x 60 - 0.5° latitude-longitude grid was centered on each of the intersection coordinates rounded to the nearest 0.5°. The number of regions meeting the following criteria were determined for each selected intersection: *VZA* difference < 7.5°, *RAZ* difference < 15°, and no sunglint. All regions with *SZA* > 72° and fewer than 20 matches were rejected. NOAA-14 was launched in Dec. 1994 with a 1340 ECT and gradually precessed to an ECT of 1705 by August 1, 2001. The typical *SZA* for the matched regions varied from ~40° in 1998 to almost 70° in 2001. Fits based on the later datasets with higher *SZA*s have smaller dynamic ranges and more scatter about the regression line.

Monthly scatter plots of NOAA-14 counts and VIRS radiances were fitted using the force-fit and PC regression methods. Figure 3 shows the resulting points

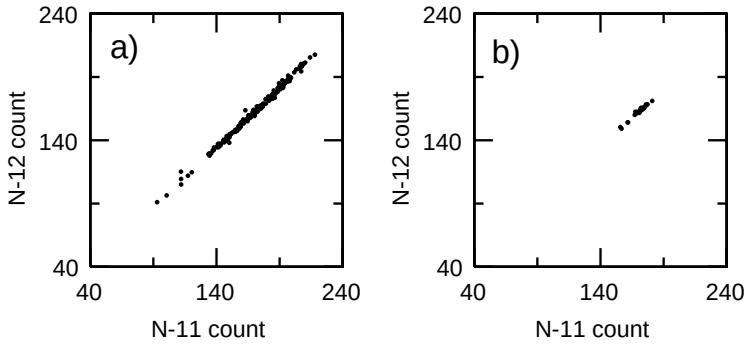

Fig. 1. a) A scatter plot of the NOAA-11 and NOAA-12 channel 1 count of cross & along track (off nadir) points for the month of Dec. 1991. b) same as a) except for nadir points only.

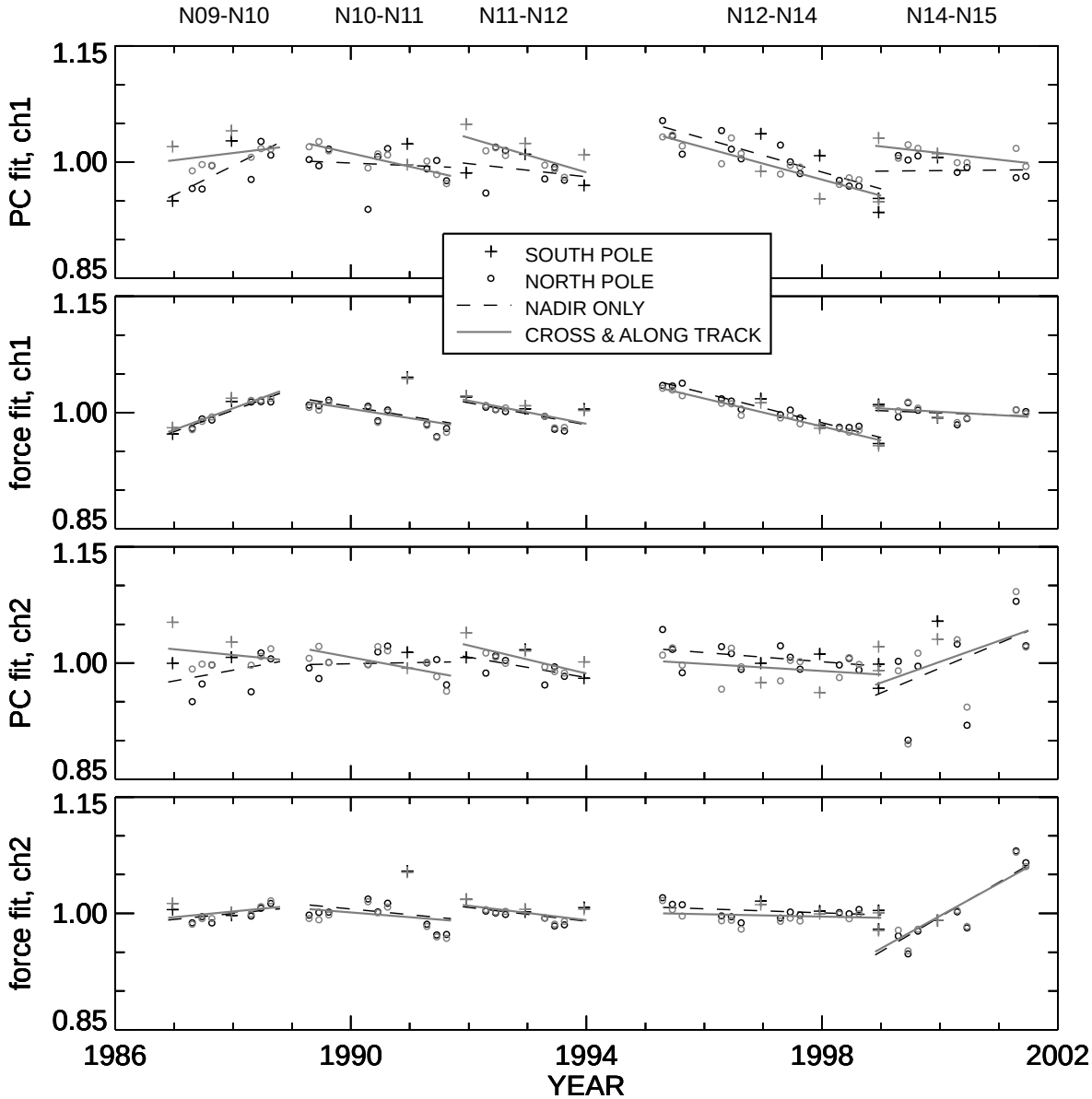

Fig. 2. The relative gain ratio of the two NOAA satellites, which are labeled on top, based on monthly regressions using the PC and force fit method for channels 1 and 2. The trend lines are also plotted. Cross & along track points and the associated trend line are shown in solid gray.

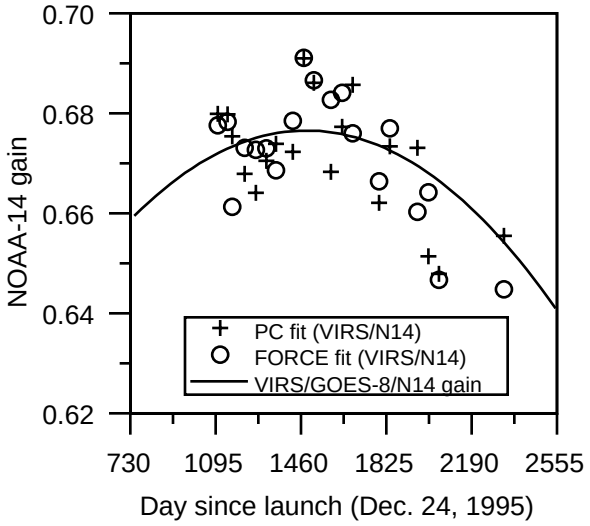

Fig. 3. Monthly NOAA-14 AVHRR visible channel gains derived from VIRS as a function of time. The VIRS/GOES-8/NOAA-14 trend line is shown.

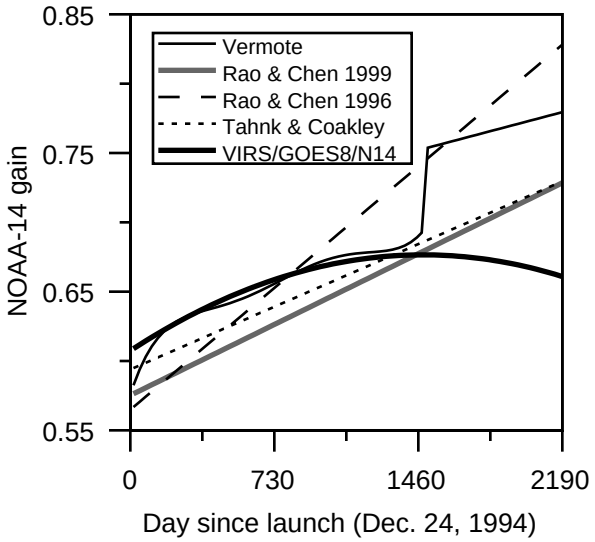

Fig. 4. Comparison of NOAA-14 AVHRR visible channel gains as a function of time.

and the NOAA-14 gain as derived from cross-calibrating VIRS with GOES-8 and GOES-8 with NOAA-14 (Nguyen et al. 2001). The monthly points follow the same type of trend as the GOES-8 based fit, thus validating the three-way circular calibration. The gain from both the points and trend line decreases after mid-2001. This behavior may be a result of the decreasing dynamic range or to some actual changes in the instrument. This trend needs further examination.

The NOAA-14 gain trend line is compared with other estimates in Fig. 4. The operational calibration (Rao and Chen 1996) was used until November 1998 when Rao and Chen (1999) provided a revised version. The coefficients are available at the web site noted earlier. The trend line from Tahnk and Coakley (2001) is based on the radiometrically stable ice sheet of Antarctica as "truth". The Vermote and El Saleous (1999) fit is based on clear ocean and cloud views. This fit can be found at http://www.dar.csiro.au/rs/CalWatch. Most of the gains are close to each other until 1999, and then diverge. The gains derived here are the only ones that decrease after 2000, but they are also the only ones with data taken after 1999. The VIRS/GOES-8/NOAA-14 gain is similar to that of before 1999. After 1999 an extrapolation was used for the Vermote and Saleous (1999) fit. Minnis et al. (2001) confirm the excellent agreement between the Vermote and Saleous (1999) and the VIRS-based fit using data taken during 1995. The wide range of fits seen in Fig. 4 suggest that any surface or cloud properties derived using NOAA-14 could have large uncertainties depending on the particular calibration that was used for the visible channel. Thus, it is important that the most accurate gain should be determined for the entire NOAA-14 period.

4. CONCLUDING REMARKS

This method presents a way to validate existing NOAA AVHRR visible calibrations and sequentially transfer a calibration from one satellite to the next. To further validate the derived trend lines, ATSR-2/NOAA-14 and MODIS/NOAA-14 monthly gains will also be obtained using the polar orbiting matching methods. The VIRS calibration will then be applied to all of the AVHRRs on the NOAA satellites from NOAA-9 through NOAA-16.

Acknowledgements

This research is supported by the Environmental Sciences Division of U. S. Department of Energy Interagency Agreements DE-AI02-97ER62341 and ITF-214216-A-Q1 under the ARM program.

References

Brest, C. L., W. B. Rossow, and M. D. Roiter, 1997: Update of Radiance Calibrations for ISCCP. *J. Atmos. Oceanic Technol.*, **14**, 1091-1109.

Loeb, N. G., 1997: In-flight calibration of NOAA AVHRR visible and near-IR bands over Greenland and Antarctica. *Intl Jour. Remote Sens.*, **18**, 477-490.

Minnis, P., L. Nguyen, D. R. Doelling, D. F. Young, and W. F. Miller, 2001: Rapid Calibration of operational and research meteorological satellite imagers, Part 1: Use of the TRMM VIRS or ERS-2 ATSR-2 as a reference. Submitted to *J. Atmos. Oceanic Technol.*

Masonis, S. J., and S. G. Warren, 2001: Gain of the AVHRR visible channel as tracked using bidirectional reflectance of Antarctic and Greenland snow. *Intl Jour. Remote Sens.*, **22**, 1495-1520.

Nguyen, L., P. Minnis, J. K. Ayers and D. R. Doelling, 2001: Intercalibration of meteorological satellite imagers using VIRS, ATSR-2 and MODIS. *Proc. AMS 11th Conf. Satellite Meteorl. Oceanogr.,* Madison, WI, Oct. 12-16.

Rao, C. R. N., and J. Chen, 1996: Post launch calibration of the visible and near-infrared channels of the Advanced Very High Resolution Radiometer on the NOAA-14 spacecraft. *Intl Jour. Remote Sens.*, **17**, 2743-2747.

Rao, C. R. N., and J. Chen, 1999: Revised post-launch calibration of the visible and near-infrared channels of the Advanced Very High Resolution Radiometer on the NOAA-14 spacecraft. *Intl Jour. Remote Sens.*, **20**, 3485.

Tahnk, W. R. and J. A. Coakley, Jr., 2001: Improved calibration coefficients for NOAA-14 AVHRR visible and near-infrared channels. *Intl Jour. Remote Sens.*, **22**, 1269-1283.

Vermote, E. and N. Z. El Saleous, 1999: private communication.